machines

MDPI

Article

Accuracy Analysis of Complex Transmission System with Distributed Tooth Profile Errors

Min Zhang [1], Zhijing Zhang [1,*], Jian Xiong [1,2] and Xiao Chen [1]

[1] School of Mechanical Engineering, Beijing Institute of Technology, Beijing 100081, China; m.zhang@bit.edu.cn (M.Z.); cielo@bit.edu.cn (J.X.); chenxiao@bit.edu.cn (X.C.)
[2] EPSRC Future Metrology Hub, University of Huddersfield, Huddersfield, Queensgate HD1 3DH, UK
* Correspondence: zhzhj@bit.edu.cn

Abstract: Tooth profile errors are the internal excitations that cause gear meshing errors, which are critical error factors affecting gear transmission accuracy. In existing studies, it is usually regarded as a constant or random distribution function. However, the actual machined tooth profile error is not a constant, so this estimation is inconsistent with the actual situation, resulting in an inaccurate evaluation of transmission accuracy. This paper proposes a method for representing tooth profile errors using distribution errors (including systematic and random errors), and a mathematical model of distributed tooth profile errors is presented. The contact stresses of the complex transmission system were compared with those obtained by formulas, proving that tooth profile errors increase contact stress. A method for calculating gear meshing error is proposed to evaluate the actual output accuracy of the complex transmission system. Compared with the test, the output accuracy is reduced by 13.8% under the temperature environment and distributed tooth profile errors. The proposed methods can accurately predict the transmission accuracy of precision transmission systems at the design stage and provide theoretical support for reducing systematic and random errors at the gear machining stage.

Keywords: complex transmission system; distributed tooth profile error; gear meshing error; transmission accuracy; contact stresses

check for updates

Citation: Zhang, M.; Zhang, Z.; Xiong, J.; Chen, X. Accuracy Analysis of Complex Transmission System with Distributed Tooth Profile Errors. *Machines* **2024**, *12*, 459. https://doi.org/10.3390/machines12070459

Academic Editors: Hermes Giberti and Raul D. S. G. Campilho

Received: 16 May 2024
Revised: 28 June 2024
Accepted: 3 July 2024
Published: 6 July 2024

Copyright: © 2024 by the authors. Licensee MDPI, Basel, Switzerland. This article is an open access article distributed under the terms and conditions of the Creative Commons Attribution (CC BY) license (https://creativecommons.org/licenses/by/4.0/).

1. Introduction

Transmission accuracy is one of the important indexes for evaluating the performance of gear transmission, usually expressed by transmission error, which can reflect the accuracy and stability of gears in transmitting motion and power. As pointed out in [1], the difference between the transmission accuracy of the gear system and the ideal accuracy is unavoidable due to multiple sources of errors in the machining process, such as manufacturing errors, workpiece mounting errors, and the transmission chain errors of the machine tool. Therefore, the existing research on transmission error mainly focuses on how to accurately determine the transmission error under the influence of load, error, friction, thermal deformation, and other parameters [2,3], as well as how to reduce the transmission error through design and machining [4–8]. Among them, they aim to improve the gear profile by modification techniques to reduce the transmission error. There has been considerable research on tooth profile modification techniques. Accordingly, in the author's previous work [9], a study on the quantitative influence of tooth pitch error, gear runout error, and assembly error on transmission error was carried out. However, as a mechanism relying on the sliding and rolling of teeth of non-trivial geometries [10], the contact state of the tooth surfaces is greatly affected by the tooth profile error. Therefore, analyzing gear transmission accuracy by considering tooth profile errors is necessary, especially regarding the effect of distribution errors of tooth profiles on transmission error. It is also a problem that the authors have been trying to study.

Gear dynamics has received increasing attention since Tuplin first proposed the spring–mass vibration model [11]. Many investigations have focused on tooth profile errors from the perspective of dynamic equations [12–16], in which tooth profile errors are regularly incorporated into dynamic equations as displacement-type functional excitations occurring at interfaces to form the unloaded static transmission error (STE). For instance, in [12], the author regarded the tooth profile error as a random tooth profile error and incorporated it into a nonlinear random model. On the other hand, Liu [17] simulated the tooth profile error excitation with pseudo-random numbers. Concerning the tooth flank error, Yuan's work [18,19] involved the distributed tooth flank error, but only the meshing clearance was considered as the distributed tooth flank error. The effect of tooth profile error on transmission error was analyzed using the above method.

Some other existing literature has addressed tooth profile errors in terms of gear tolerances, thin slice gears, and undesired tooth profile errors [20–24], e.g., of which [20], manufacturing errors were treated as random errors. Thus, a random tooth profile error distribution was given for each tooth. In [21,22], the tooth profile deviation distribution was obtained by discretizing the teeth. In [23,24], the authors focused on the effect of tooth profile error on meshing stiffness. The former defined the tooth profile error as the amount of tooth profile modification, while the latter represented the tooth profile error as the sum of the sinusoidal curves. In the calculation, the amplitude was given by the determined value.

The abovementioned research on tooth profile errors needs to be revised, and the current understanding of gear errors still needs to be completed. Recently, in another research field, the study of evaluating the transmission errors of harmonic reducers for robotics based on actual machined tooth profiles has attracted the authors' attention. For this paper, the tooth profiles of the harmonic drive were measured using a commercial non-contact CMM, the pitch errors were extracted using various mathematical methods, and the angular transmission error of the harmonic drive was predicted considering three-dimensional tooth engagement [25]. The above study predicts that the prediction of transmission errors based on actual machined tooth profiles becomes the future trend for research and improvement of transmission errors, regardless of spur or harmonic gearing.

Therefore, this paper aims to simulate the effect of actual machining errors on tooth profile errors, including position errors and form errors according to the characteristics of precision machinery manufacturing, and then assess the impact of such distributed tooth profile errors on the transmission error of the complex transmission system. First, the mathematical modeling method is used to simulate the tooth profile slope deviation (positional error) caused by systematic errors and the tooth profile form error caused by random errors in gear machining errors, making the obtained involute tooth surface as close as possible to being in line with the actual. Secondly, the effects of distributed tooth profile errors on contact stresses are evaluated based on the established three-dimensional solid model containing distributed tooth profile errors and finite element dynamics calculations. Furthermore, the evaluation method of gear meshing error is proposed, which provides an effective method for evaluating the transmission accuracy of the gear transmission system. Finally, based on the purpose of obtaining the three-dimensional point cloud data of the actual tooth surface, a general-purpose contact CMM was used to measure the experimental gears and finite element calculations were carried out on the experimental gears, which verified the significance of the involute tooth profile error modeling in this paper.

This paper is organized into six sections. Section 2 contains the involute profile error modeling, including systematic and random errors. Section 3 uses the finite element dynamics method to calculate the complex transmission system with distributed tooth profile error. The effects of distributed tooth profile errors on the contact stress and gear meshing errors are determined. The experiment in Section 4 verifies the presented approach's validity. Section 5 discusses the benefits of the proposed methods in this paper. Section 6 concludes this paper.

2. Geometric Model of Complex Transmission System Containing Distributed Tooth Profile Errors

This paper takes the complex transmission system of the joint for a large space manipulator as the research object. The reason is that as an essential transmission of the joint, its planetary drive has many stages and large gear ratios. In addition, the space environment and stress state differ from the ground environment. Gear tooth profiles for the complex transmission system are all involutes. Their manufacturing methods include molding, profiling, and generating. Currently, the most commonly used method is generating, such as gear shaping, hobbing, and shaving, of which the first two are the most widely used gear processing methods. The factors that affect gear machining accuracy include errors in machine tools, cutting tools, gear blanks, and mounting. These errors affect the accuracy of the processed gear according to a specific law. For example, machining errors in hobbing can lead to six profile errors: flanks out of the edge, asymmetry, profile angle error, periodic error, root cutting, and root fillet error. Figure 1a shows the asymmetry of tooth profile (also called skewed teeth) generated during gear hobbing, which is formed due to the following factors. Note the poor radial performance of the hob blade after grinding, that is, the rake angle of the hob blade is not equal to zero, which results in non-radial error γ of the front blade, as shown in Figure 1b.

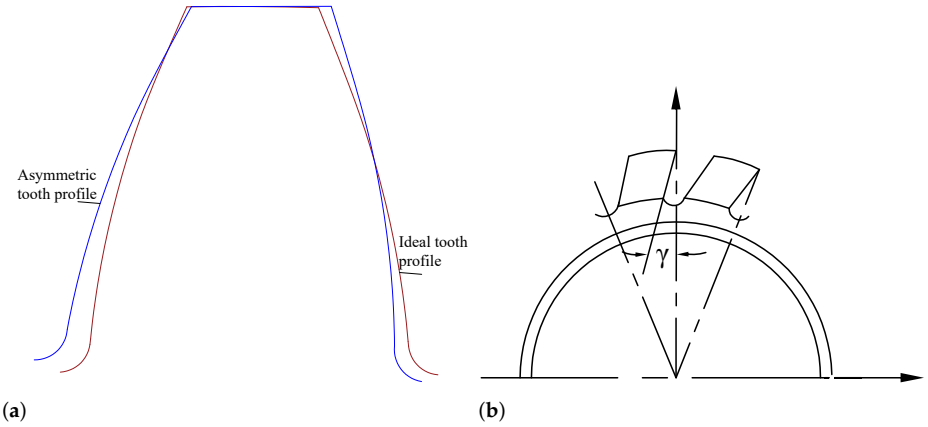


Figure 1. Formation of skewed teeth. (**a**) Tooth profile asymmetry. (**b**) Positive rake angle.

Therefore, the actual tooth profile deviates from the ideal form, and the actual gear is not an ideal involute gear. However, the gear system mainly relies on the contact meshing of the tooth surface to transmit motion and power, and the contact state between two tooth surfaces is greatly affected by the tooth profile error. For a high-precision complex transmission system, the meshing excitation due to tooth profile errors will be a crucial factor affecting the transmission accuracy. Accordingly, this section establishes a three-dimensional solid model of the complex transmission system with distributed tooth profile errors through the modeling and analysis of tooth profile errors, providing a three-dimensional geometric model for the subsequent finite element analysis in this paper.

2.1. Modeling of Involute Tooth Profile Error

Given the above analysis, the machining error that forms tooth profile error can be composed of systematic and random errors. The geometric error of the tooth surface caused by systematic error is deterministic, which can describe the distribution law of the geometric error produced by the same machining process. In contrast, random errors lead to differences between machined gears. Therefore, to establish an involute cylindrical gear that matches the machining error, we divided the involute tooth profile error into systematic and random errors in the subsequent modeling and provided their modeling formulas, respectively.

In the design of involute gears, tooth profile accuracy is one of the items used to evaluate the accuracy of the tooth flanks on the same side of the gear teeth. It is generally expressed by the total deviation ΔF_α of the tooth profile. As presented in Figure 2, the total deviation of tooth profile refers to the distance between the two design tooth profile traces encompassing the actual tooth profile trace within the range of the profile count [26]. To satisfy the requirements of transmission stability, the total deviation is specified to follow the condition [27]:

$$\Delta F_\alpha \leq F_\alpha \tag{1}$$

where F_α is the total tolerance value of the tooth profile, which is determined according to the design requirements.

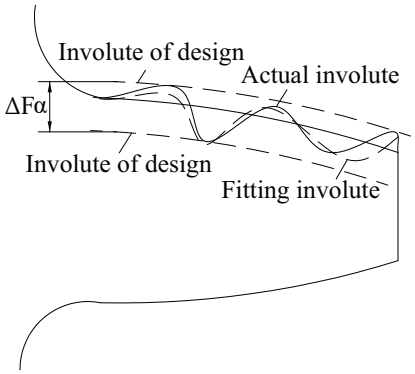


Figure 2. Schematic diagram of involute tooth profile.

The total deviation of the tooth profile can be decomposed into two parts, expressed by the tooth profile form error representing the form accuracy and the tooth profile slope deviation representing the direction accuracy, respectively. Tooth profile form error is mainly formed by high-frequency vibration of the machining system and the form error of the cutting tool of the forming gear. Tooth profile slope deviation, also known as pressure angle deviation, is related to the hob cutter's pressure angle, the base circle's diameter deviation, and the gear workpiece's geometric eccentricity during the cutting process. Consequently, in gear machining, systematic errors mainly cause tooth profile slope deviation, while random errors mostly form tooth profile form errors. The mathematical models of the systematic and random errors that form the involute tooth profile errors will be described in detail as follows.

Figure 3 refers to the formation of the actual tooth flank, where Figure 3a is the formation of the involute curve, and its polar coordinate equation takes the form of:

$$\begin{cases} r_k = \frac{r_b}{\cos \alpha_k} \\ \theta_k = \tan \alpha_k - \alpha_k \end{cases} \tag{2}$$

where r_b is the radius of the base circle and r_k refers to the radius vector of point k on the involute. The θ_k denotes the development angle, which is a function of the pressure angle α_k of point k. Since the pressure angles at each point on the involute are unequal, a change in α_k will lead to a variation in θ_k. Therefore, the involute position error e_p caused by systematic errors in the machining process can be expressed as a function of the change in pressure angle $\Delta\alpha_k$.

$$e_p = \Delta r_k(\Delta\alpha_k) \tag{3}$$

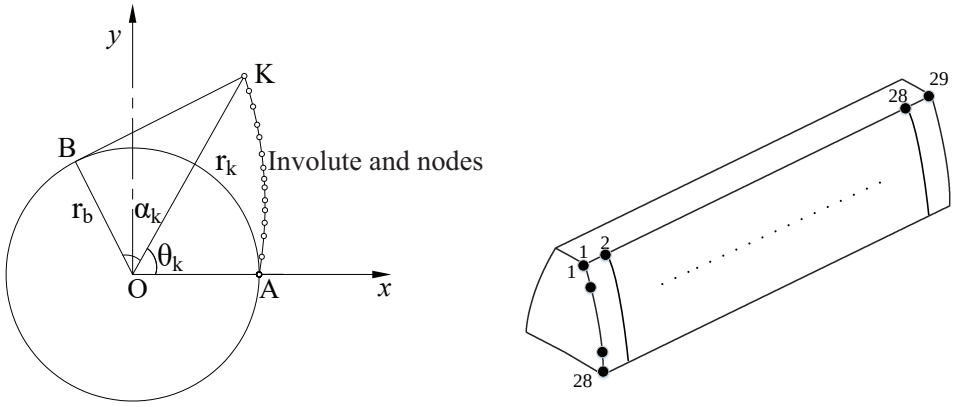


Figure 3. Formation of actual involute tooth flank. (**a**) Involute tooth profile curve. (**b**) Involute tooth flank.

That is, the actual radial vector $r_k{}'$ is as follows:

$$r_k{}' = r_k + \Delta r_k(\Delta\alpha_k) \tag{4}$$

In practice, we usually calculate the variation in the pressure angle α on the pitch circle, which is also the tooth profile angle error $\Delta\alpha$. It can be obtained by combining Equation (5) with Equation (6).

$$L_\alpha = 0.92 \times \left(\sqrt{r_a^2 - r_b^2} - r_b \tan\alpha + \frac{h_a^* m}{\sin\alpha} \right) \tag{5}$$

where L_α is the range of values for evaluating tooth profile deviation, r_a refers to the radius of the addendum circle, h_a^* denotes the addendum coefficient, and m is the modulus of the gear.

$$\Delta\alpha = -\frac{\Delta f_\alpha}{L_\alpha \tan\alpha} \tag{6}$$

where Δf_α is the tooth profile slope deviation.

Then, the point cloud data (x',y',z) on the involute containing the systematic errors can be obtained by converting the polar coordinates into Cartesian coordinates.

On the other hand, the theoretical parameter equation of an involute is given as follows:

$$\begin{cases} x = r_b \cos\theta + r_b\theta \sin\theta \\ y = r_b \sin\theta - r_b\theta \cos\theta \end{cases} \tag{7}$$

where θ refers to the rolling angle at any point of the involute, which can be computed by $\theta{=}\theta_k + \alpha_k$; thus, the tooth profile form error caused by random errors can be expressed as:

$$\begin{cases} \Delta x = \Delta r_b \cos(\Delta\theta) + \Delta r_b \Delta\theta \sin(\Delta\theta) \\ \Delta y = \Delta r_b \sin(\Delta\theta) - \Delta r_b \Delta\theta \cos(\Delta\theta) \end{cases} \tag{8}$$

When calculating, it is assumed that the variation Δr_b in the radius of the base circle and the variation $\Delta\theta$ in the rolling angle follow a normal distribution.

$$\begin{cases} \Delta r_b \in \mathrm{N}\left(\mu_{\Delta r_b}, \sigma_{\Delta r_b}\right) \\ \Delta\theta \in \mathrm{N}(\mu_{\Delta\theta}, \sigma_{\Delta\theta}) \end{cases} \tag{9}$$

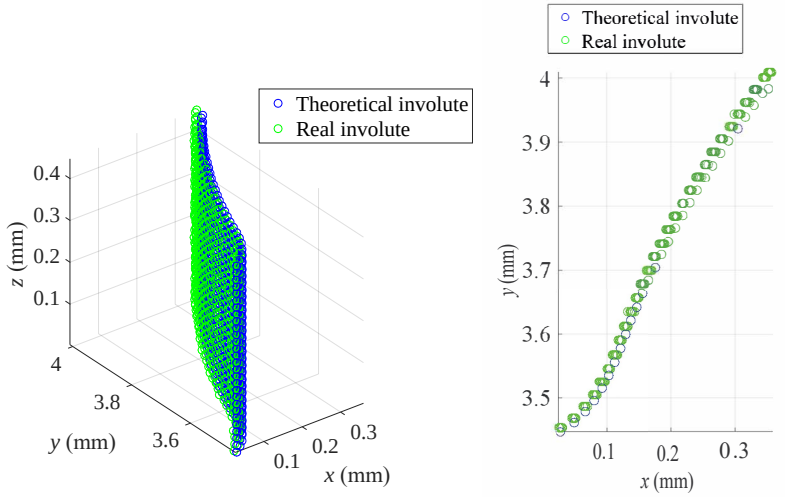
where $\mu_{\Delta r_b}$ and $\mu_{\Delta\theta}$ are the mean values of the variation in the base circle radius and the variation in rolling angle, respectively. $\sigma_{\Delta r_b}$ and $\sigma_{\Delta\theta}$ are their standard deviations, respectively.

Accordingly, the points (X',Y',Z) on the actual involute are determined by the following formula under the combined action of systematic and random errors.

$$\begin{cases} X' = x' + \Delta x \\ Y' = y' + \Delta y \\ Z = z \end{cases} \tag{10}$$

2.2. Generation of Error Tooth Surface

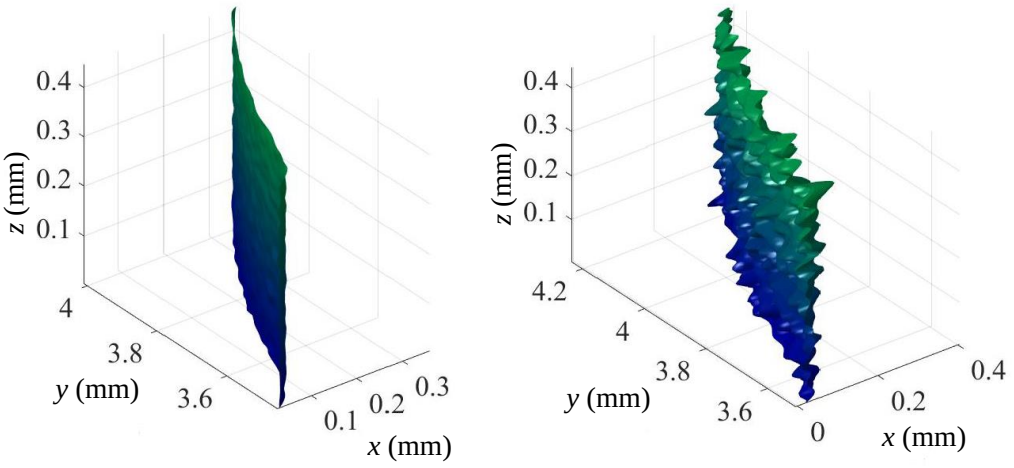
Figure 3b displays a tooth flank with 28 points along the involute direction and 29 involutes along the face width direction. When using the above equations to generate error tooth flanks that include tooth profile errors, the first problem to be solved is to determine the point cloud data for the $m \times n$ matrix. The specific steps are detailed below. In the first step, the first theoretical involute curve is acquired using Equation (7), and the (x_0, y_0, z_0) coordinates of the m points are obtained. It is worth noting that the z coordinate of the first involute is 0, and then n such involutes are determined along the z direction of the face width. Subsequently, combined with Equation (2) to Equation (6), the data matrix of $m \times n$ considering systematic errors is determined. Furthermore, random errors can be obtained by combining Equation (8) with Equation (9), thus determining the point cloud data on the actual tooth flanks based on Equation (10). The results are plotted in Figure 4a. To better compare the ideal and error points, their xy views are depicted in Figure 4b.



(**a**) (**b**)

Figure 4. Comparison between ideal and error points. (**a**) Ideal and error points. (**b**) xy view of ideal and error points.

Zhang [28] used NURBS surface reconstruction to represent geometric error. However, in the case of gears, the establishment of error surfaces based on NURBS numerical modeling has yet to be thoroughly studied. Hence, for the generated point cloud data, this paper creatively uses the NURBS numerical model for the first time to establish an error surface for gears with distributed tooth profile errors, as depicted in Figure 5. Among them, Figure 5b is the tooth flank magnified ten times along x and y, respectively, to display the form error of the tooth profile.



(**a**) (**b**)

Figure 5. Actual involute tooth flank and its error amplified. (**a**) Interpolated 3D surface. (**b**) Error amplified.

2.3. Verification of Surface Modeling Accuracy

The distance d between the set of points on the actual involute surface and the set of points on the theoretical involute surface is used to verify that the geometric error of the tooth profile is within the total profile tolerance.

$$d = \sqrt{(x_i - x_{0i})^2 + (y_i - y_{0i})^2} \tag{11}$$

where (x_i, y_i) are points on the actual involute surface and (x_{0i}, y_{0i}) represent points on the theoretical involute surface.

Based on Equation (11), the maximum value d_{Max} and the minimum value d_{Min} are determined, respectively, which makes the actual tooth profile errors F'_α satisfy the following condition:

$$F'_\alpha = |d_{\mathrm{Max}}| + |d_{\mathrm{Min}}| \leq F_\alpha \tag{12}$$

2.4. Geometric Model Of Complex Transmission System

Based on Section 2.2, a NURBS mathematical model is employed to represent the actual tooth flanks with distributed tooth profile errors, providing a basis for integrating the error tooth flank with the CAD design model. Furthermore, the gear teeth with distributed tooth profile errors were obtained, as shown in Figure 6. The 3D geometric model of the gear containing distributed tooth profile errors was obtained using CAD modeling software (PTC Creo Parametric 3.0 M060). Finally, we obtained the geometric model of the complex transmission system, which includes a fixed-axis gear train and a planetary gear train, as shown in Figure 7. Figure 7a displays the fixed-axis gear train, which includes an input gear 1, two pinions 2, a fixed carrier, and a double gear 3. Figure 7b is the planetary gear train, which contains a gear 3′, a gear 4, a gear 5, an output gear 6, and a fixed ring 7. Figure 7a,b are connected via double gear 3. For convenience of analysis, the fixed carrier is omitted in Figure 7a. At the same time, the internal gear of gear 3 is also omitted in Figure 7b, and only the external gear 3′ is retained.

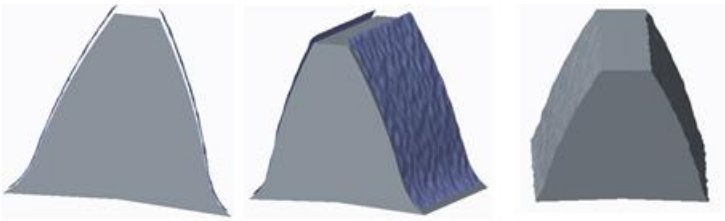
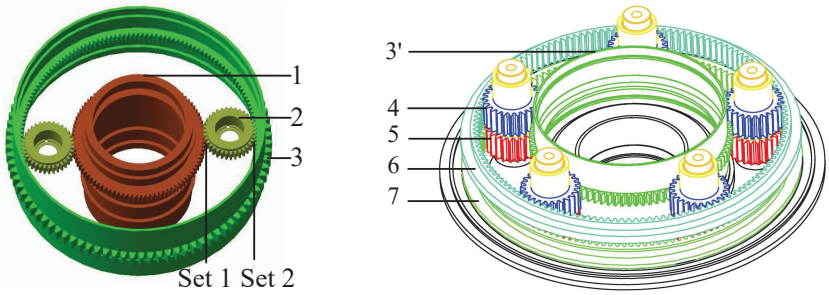


Figure 6. The gear teeth with distributed tooth profile error.

Moreover, given the sensitivity analysis in the author's previous study [9], we know that the gear errors of the planetary gear system, especially gears 4 and 5, have a significant impact on the whole transmission system. Hence, the planetary gear system is the focus of this paper. To depict the planetary gear system, the planetary carrier and output shaft in Figure 7b are omitted, but they all exist in the actual analysis. The basic parameters and profile accuracy of each gear are presented in Tables 1 and 2, respectively.



(**a**) (**b**)

Figure 7. Complex transmission system. (**a**) Fixed-axis gear train. (**b**) Planetary gear train.

Table 1. Parameters of each gear.

Gears	Module (mm)	Number of Teeth	Width (mm)	Pressure Angle (°)
Gear 1	1	91	8	20
Gear 2	1	35	9	20
Gear 3	1	161	8	20
Gear 3′	2	90	11	20
Gear 4	2	25	24	20
Gear 5	2	24	24	20
Gear 6	2	140	22	20
Gear 7	2	139	22	20

Table 2. Profile accuracies of each gear.

Gears	Tooth Profile Tolerance (μm)	Tooth Profile Form Error (μm)	Tooth Profile Slope Deviation (μm)	Tooth Line Tolerance (μm)
Gear 1	8.5	6.5	5.5	9
Gear 2	7.5	5.5	4.6	9
Gear 3′	10	7.5	6	9
Gear 3	14	11	9	11
Gear 4	7.5	5.5	4.6	9
Gear 5	7.5	5.5	4.6	9
Gear 6	14	11	9	11
Gear 7	14	11	9	11

3. Finite Element Dynamic Model

The primary purpose of this section is to analyze the contact dynamics of the planetary gear system under the combined effect of distributed tooth profile error, load, and temperature field. Accordingly, the contact analysis should be performed in two steps. First, a finite element dynamic model is developed using Dynamic/Explicit. Second, the contact stress and gear meshing error are determined based on the simulation results. As for dynamic analysis, the masses and inertias of the wheels are shown in Table 3. The preprocessing settings for the finite element model are reported in Table 4.

Table 3. Masses and inertias of each gear.

Gears	Masses (Kg)	Inertias (Kg· mm^2)
Gear 1	0.448	819
Gear 2	0.041	11.1
Gear 3	1.236	7070
Gear 3′	1.236	7070
Gear 4	0.7	356
Gear 5	0.645	356
Gear 6	1.797	31,100
Gear 7	1.309	25,300

Table 4. Finite element preprocess settings.

Modeling Steps	Parameters	Numerical Value
Solver settings	Software	ABAQUS (Abaqus/CAE 2021)
	Step	Dynamic
	Solver	Explicit
Mesh	Element	C3D8R
Property	Ultra-high-strength stainless steel (gear)	Young's modulus 190 GPa
		Poisson's ratio 0.305
		Mass density 7.9 g/cm^3
		Expansion coeff 1.1 × 10^{-5}
	Titanium alloy (carrier and shaft)	Young's modulus 105 GPa
		Poisson's ratio 0.34
		Mass density 4.51 g/cm^3
		Expansion coeff 1.09 × 10^{-5}
Interaction	Interaction	Surface-to-surface contact (Explicit)
	Interaction property	Coulomb friction coeff 0.1 and hard contact
	Constraints	Coupling and tie
Boundary condition	Temperature	From −20°C to 50°C
	Fixed boundary	Bottom of support
	Rotate or translate	Gears and shafts

3.1. Influence of Distributed Tooth Profile Error on Contact Stress

First, we illustrate the influence of distributed tooth profile error on the gear contact stress by using the example of the fixed-axis gear train of the complex transmission system. The idea is to use the gear contact stress calculation method given in Section 4.1.2 of the national standard GB/T 3480-1997 [29] to obtain the calculated contact stress. However,

this must not take into account the distributed tooth profile error. Then, the above results are compared and analyzed with those obtained by the finite element calculation.

Whether Hertz's contact theory [30] or the national standard is applied to calculating the contact stress of involute cylindrical gears, the effect of temperature on the contact stress is not considered. Therefore, the temperature field was not considered in the finite element dynamic model of the error model of the fixed-axis gear train. For comparison, Table 5 shows the calculated contact stresses obtained based on the formulas and the maximum contact stresses obtained by finite element analysis.

Gear meshing is a line contact that starts from the tooth root of the driving gear pushing the tooth tip of the driven gear. Therefore, the driving gear's root and the driven gear's tip are prone to stress concentrations. In addition, when the gears are just coming into a mesh, or the single and double teeth alternately mesh, the maximum value of the stress variation is easily reached.

Table 5. Comparison of calculated contact stresses with maximum contact stresses of FEM.

Parameters		Calculated Contact Stress (MPa)	FEM (MPa)	Relative Error (%)
Set 1	Gear 1	557.8427	619.4	11.03
	Gear 2	572.0677	559.2	2.25
Set 2	Gear 2	458.9514	426.8	7.53
	Gear 3	458.9514	556.6	18.99

Table 5 clearly shows that the numerical results for gears 1 and 3 are larger than those calculated by the formulas, with relative errors of 11.03% and 18.99%, respectively. The reason is that the stress concentration occurs on the root of gear 1 and the tip of gear 3. On the other hand, the finite element dynamic model considers the distributed tooth profile error, so the local contact stress is larger than those calculated by formulas. More importantly, the calculated contact stress can only evaluate the stress-bearing limit of the gear as a whole, whereby it cannot obtain the stress concentration point and the maximum contact stress when the stress concentration occurs. In contrast, the FEM is closer to the actual situation of the gear system. Consequently, when designing gears, we should consider the distribution of tooth profile error on the whole tooth surface rather than simply determining the gear's bearing limit based on an ideal geometric model or a fixed formula.

3.2. Influence of Distributed Tooth Profile Error on Transmission Accuracy

In the space environment, many factors affect the joint's output accuracy and operation stability, such as the temperature field, load, and parts errors. After we have analyzed and proved that the distributed profile errors significantly impact the contact stress of the gear train, we need to analyze the transmission accuracy of the complex transmission system under the effects of distributed profile error, temperature, and load. In addition, we propose a method to obtain the meshing errors by combining the finite element analysis results. Then, at the end of this section, based upon the author's previous work on this large space manipulator [9], the output accuracy and stability of this large space manipulator in the actual service process are comprehensively evaluated.

As depicted in Figure 8, it is a meshing pair of involute tooth profiles. When the pair of tooth profiles engage at any position, the common normal line passing through the contact points is the same line N_1N_2, which indicates that all the engagement points of the pair of involute tooth profiles from engagement to disengagement are on this line. Therefore, line N_1N_2 is the trajectory of the contact points of the tooth profile in a fixed plane, also known as the line of action.

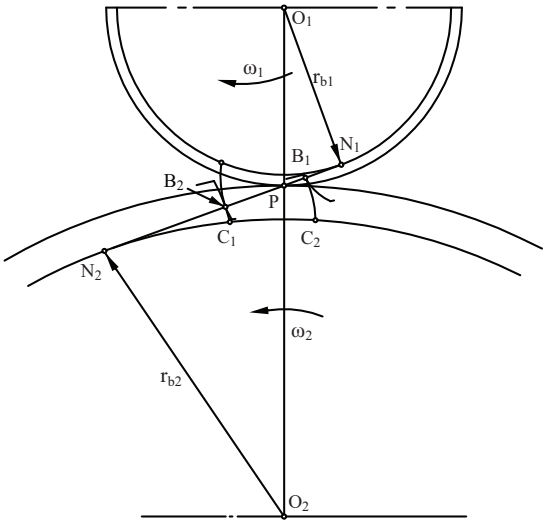


Figure 8. Meshing diagram of involute tooth profile: O_1O_2 is the two gears' centerline; P is the intersection of O_1O_2 and N_1N_2; B_1B_2 is the actual line of action; r_{b1} and r_{b2} are the gears' base circle radius, and ω_1 and ω_2 are their angular velocities; C_1 and C_2 are the two gears' starting points of the involute curves.

Subsequently, the coordinates of all nodes on the involute where the maximum contact stress occurs are extracted according to the principle of invariant positive pressure direction of the involute tooth profile. Based on the original node coordinates and the deformed node coordinates, the radius of the circle where each node on the involute is located is obtained, which corresponds to the radial r_k forming the involute, as presented in Figure 3a. As a result, the radius difference δr_j before and after the gear deformation can be determined. For illustration, Table 6 and Table 7 display the involute node radius changes for gears 3′ and 4, respectively.

Table 6. Change in involute node radius of gear 3′.

No Temperature			With Temperature		
Before Deformation (mm)	**After Deformation (mm)**	**Radius Difference (mm)**	**Before Deformation (mm)**	**After Deformation (mm)**	**Radius Difference (mm)**
87.50001	87.50137	0.001361	87.49996	87.50254	0.002589
87.96042	87.9628	0.002373	87.96038	87.96388	0.003504
88.41834	88.42083	0.002494	88.41836	88.42268	0.004324
88.87398	88.87638	0.002402	88.87395	88.87846	0.004508
89.32725	89.32971	0.002463	89.32725	89.33252	0.005268
89.77824	89.77896	0.000716	89.77831	89.7825	0.004185
90.22696	90.22597	−0.00099	90.227	90.23014	0.003144
90.67344	90.67352	7.72×10^{-5}	90.67351	90.67691	0.003402
91.11783	91.11916	0.001337	91.11783	91.12363	0.005799
91.56003	91.56075	0.000724	91.56	91.56513	0.005124
92.00001	92.0012	0.001194	92.00003	92.00616	0.006127

Since the gear meshing error occurs along the line of action, i.e., the normal direction of the involute tooth profile, the following formula can determine the gear meshing error. The pressure angle α_k and the development angle θ_k can be determined by Equation (2).

$$\delta = \delta r_j \cdot \theta_k \tag{13}$$

Table 7. Change in involute node radius of gear 4 when gear 4 is meshed with gear 3′.

No Temperature			With Temperature		
Before Deformation (mm)	**After Deformation (mm)**	**Radius Difference (mm)**	**Before Deformation (mm)**	**After Deformation (mm)**	**Radius Difference (mm)**
23.8238	23.90013	0.076329	24.2386	24.33186	0.093254
24.23868	24.30746	0.06878	24.64855	24.72476	0.076204
24.64866	24.69927	0.050611	25.0533	25.11462	0.061315
25.05332	25.08933	0.036009	25.45233	25.49516	0.042833
25.45229	25.46973	0.017433	25.8455	25.86815	0.022646
25.84553	25.84219	−0.00334	26.23244	26.23121	−0.00123
26.23242	26.20512	−0.02729	26.61312	26.5875	−0.02562
26.61316	26.56096	−0.0522	26.98747	26.93468	−0.05279

Combining the radius difference δr_j of the involute node with Equations (2) and (13), it is possible to determine the meshing errors for each pair of gears under the excitation of distributed profile error, rotational speed, and external load in the absence and presence of temperature variations, as illustrated in Figures 9–11.

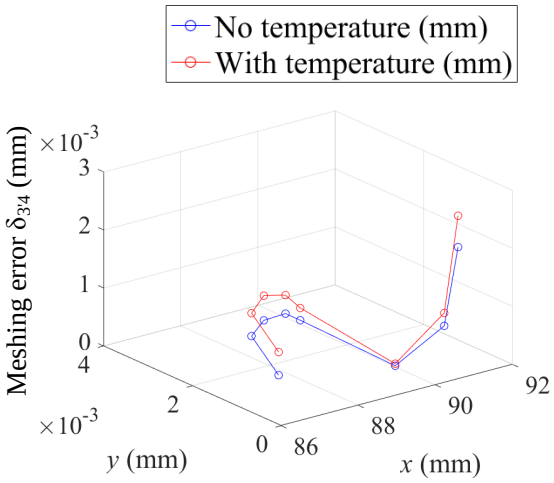


Figure 9. Meshing error of gears 3′ and 4.

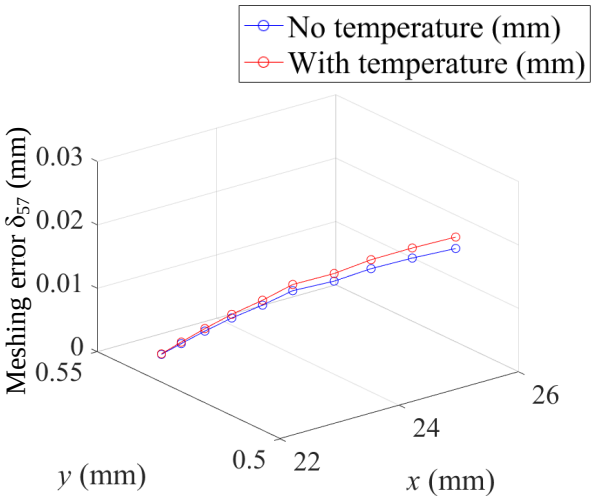


Figure 10. Meshing error of gears 5 and 7.

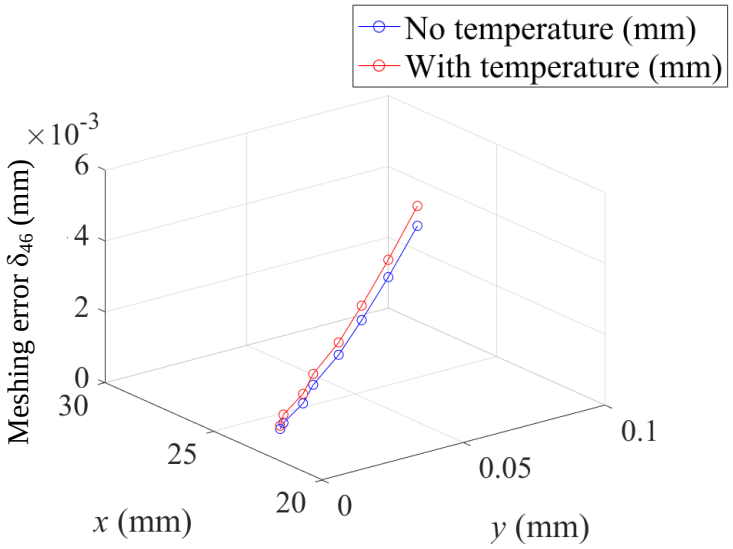


Figure 11. Meshing error of gears 4 and 6.

Because two gears are involved at each meshing point location, the position coordinates xy of the meshing points are used to represent the node positions. The z coordinates of Figures 9–11 represent the meshing errors. The relationship between the position of the meshing points and the meshing errors is clearly illustrated.

Referring to Figures 9–11, it can be observed that regardless of temperature, the tooth profile errors will affect the variation in the transient ratio in the gear mesh transmission, i.e., it causes the variation in the transient transmission error, which is the reason why the tooth profile error is an internal excitation of the gear transmission. To minimize this internal excitation, it is necessary to make the tooth surfaces in uniform contact as much as possible, instead of non-uniform contact. Meanwhile, the meshing errors of each pair of gears in the planetary gear system are higher than those without temperature variation, which indicates that the temperature has a significant effect on the transmission accuracy of the system.

Accordingly, in the cases of coupling tooth profile error, load, and temperature field, the transmission error of the system can be calculated through the linear displacement Equation (14) of gear meshing error.

$$\Delta\delta \cdot r_b = x \tag{14}$$

where $\Delta\delta$ refers to the angular displacement of the gears' torsional motion and r_b is the radius of the base circle.

In this work, the transmission error with the coupling factors was predicted to be 0.192′. Combined with the transmission error TE′ based on machining and assembly errors in the author's previous investigation [9], the total transmission error for the complex transmission system was 1.5021′. Compared with the experimental results on transmission accuracy in the same reference [9], it demonstrates that the joint's transmission error is 13.8% higher than that of the test due to the action of geometric errors, assembly errors, tooth profile errors, load, and temperature field.

The results prove that, under the comprehensive influence of the above error factors, the actual output accuracy of the complex transmission system of the joint for a large space manipulator is 13.8% lower than that of the test accuracy during the actual space operation. Consequently, the operation accuracy and stability of the large space manipulator in service will be seriously affected when completing the scheduled task.

4. Experiment

Since the complex transmission system studied in this paper is expensive and involves many gears, no spare objects are available for experimentation. Therefore, to explore the effect of machining error on the tooth profile error, this paper took the first-stage gear pair of a three-stage gearbox as the experimental object, as shown in Figure 12. Their basic parameters and profile accuracies are denoted in Table 8 and Table 9, respectively.

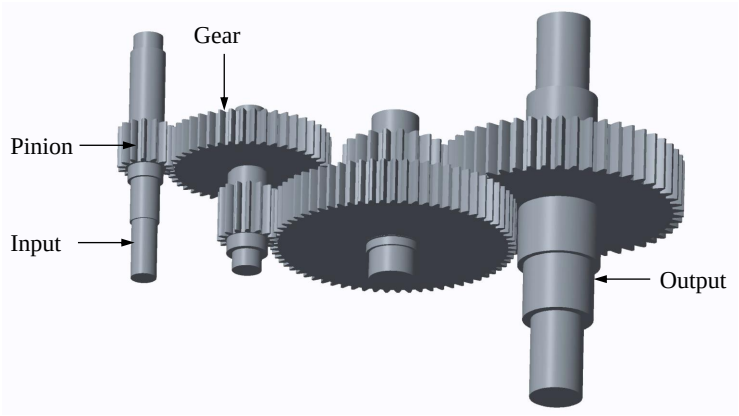


Figure 12. Three-stage gear system.

Table 8. Parameters of measured gears.

Gears	Module (mm)	Number of Teeth	Width (mm)	Pressure Angle (°)
Pinion	3	14	36	20
Gear	3	44	30	20

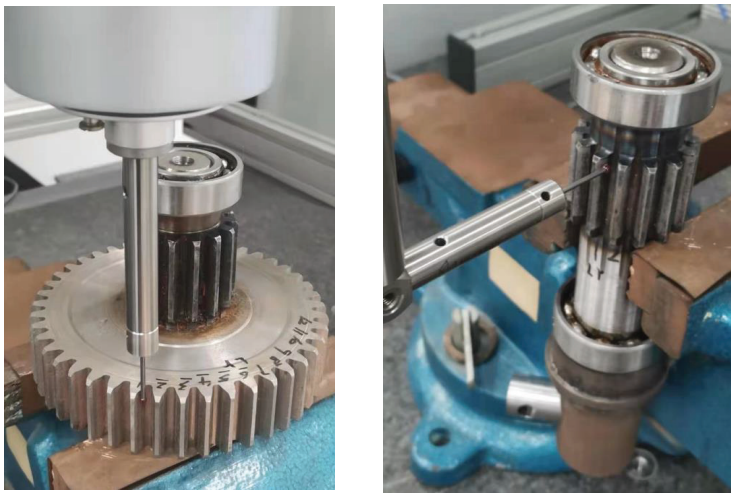
Table 9. Profile accuracies of measured gears.

Gears	Tooth Profile Tolerance (μm)	Tooth Profile form Error (μm)	Tooth Profile Slope Deviation (μm)	Tooth Line Tolerance (μm)
Pinion	20	19	15	18
Gear	25	19	15	18

4.1. Measurement of Gear Tooth Surfaces

As we all know, a special gear measuring machine is usually used for measurement after gear machining. Then, its geometric accuracy is evaluated to determine whether the machining error meets the requirements for gear accuracy. But it cannot obtain the three-dimensional point cloud data of the tooth surface. The author's team has been researching error and precision assembly technology and theory for a long time. It has accumulated many bases in obtaining the surface topography of parts, including selecting measurement methods and developing measurement strategies [28,31–34]. To compare the effects of different measurement methods on the measurement data of the assembly surface of precision machined parts, Zhang [33] designed an experimental sample and analyzed the flatness measured on the sample surface using a triggered CMM, a continuous scanning profilometer, an auto-zoom three-dimensional surface measuring instrument, and a metrological X-CT. The following conclusions were drawn: CMMs not only have the advantages of a simple calibration process, good measurement repeatability, minor systematic errors, and controllable sampling interval but also have the advantages of flexible probes, adaptable to a wide range of features, such as cylindrical and semi-circular surfaces, as well as low requirements for measurement environments. It has also been verified that the CMM is more suitable for acquiring geometric form error information. In addition, the evaluation of the advantages and disadvantages of a measurement method

mainly depends on whether it can adapt to the surface features, whether it can carry out efficient and high-precision measurements, whether it can improve measurement efficiency, and whether it can reduce the amount of data collected under the premise of guaranteeing the measurement accuracy [35]. Therefore, the measurement experiments in this section use a CMM (Brown & Sharpe Mistral 7107, with a measurement uncertainty of (1.5 + L/300) μm, the measurement system of PC-DMIS, and a 40 mm stylus with ball tip 2 mm in diameter), rather than a specialized gear measuring machine, to measure the surface topography of the experimental gears, as described in Figure 13.

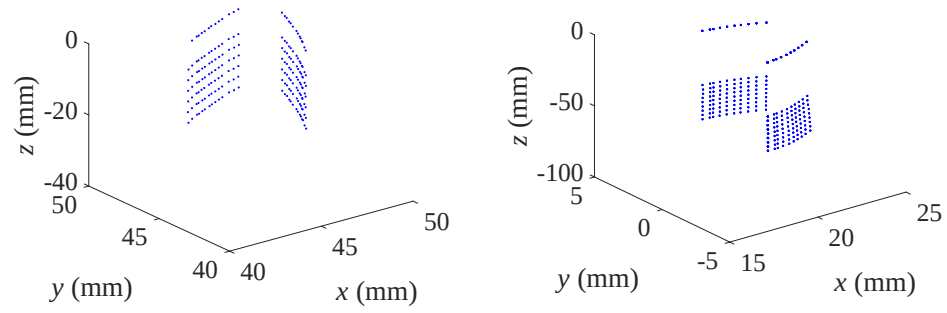


(**a**) (**b**)

Figure 13. Measurement experiment of tooth flanks. (**a**) Gear. (**b**) Pinion.

First, in developing the measurement scheme for the gear surface, the layout scheme of the measurement points is shown in Figure 3b. Furthermore, a fixed coordinate system needs to be established for the measurement, and each tooth is measured in this coordinate system. In terms of the clamping method, since several tooth surfaces of the gear need to be measured simultaneously, to facilitate one-time measurement and reduce the measurement error generated by part clamping, we need a fixture to fix the gear to ensure that it is not moved during the measurement process. Considering that the experimental gear is a gear shaft, a fixed shaft part can be used to fix the gear, so a vise was chosen for this experiment. It is undeniable that mounting a vise will introduce mounting error, which will be a part of the measurement error of the tooth surface measurement data. After obtaining the measurement data, we will process it, including gross error removal, systematic error removal, random error filtering, etc., and interpolate the measurement data points to obtain matrix data that can be modeled using NURBS surfaces.

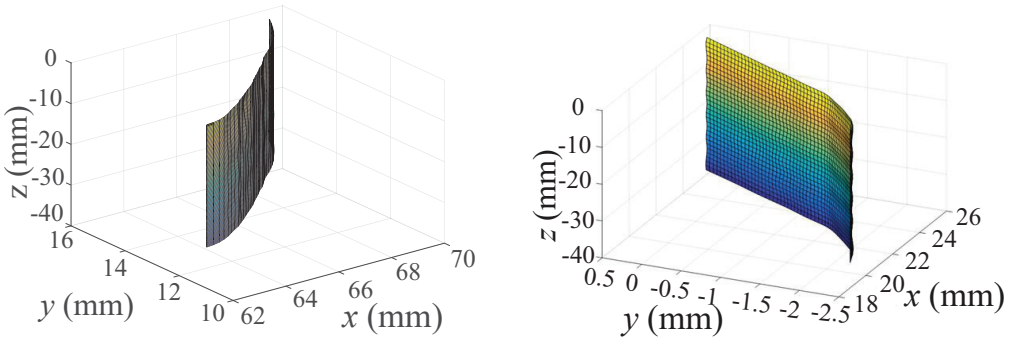
The original measurement data of the gear pair are reported in Figure 14. Generally, the accuracy of a gear is evaluated when measuring its tooth flanks. Although more parameters can be used to evaluate the geometric accuracy of gears, such as tooth pitch deviation, tooth profile deviation, helix deviation, tangential integrated deviation, one-tooth tangential integrated deviation, etc., this paper focuses on studying the impact of geometric distribution errors on the gear transmission accuracy. Therefore, after measuring the point cloud data of the tooth surface using the CMM, we are more concerned about the error distribution state of the whole tooth surface. Other geometric errors are not the focus of this paper, so they are not evaluated in this paper.



(**a**) (**b**)

Figure 14. Original measurement data of tooth flanks. (**a**) Gear. (**b**) Pinion.

In terms of the measured data, based on Section 2.2, the NURBS interpolated 3D surfaces of the actual measured gears were established, as presented in Figure 15. It can be noticed that the errors of the tooth flanks are mainly concentrated in the *y* direction, that is, the normal direction of the involute. Finally, the actual gear models with distributed tooth profile errors were determined by integrating error tooth surfaces with their CAD design models.



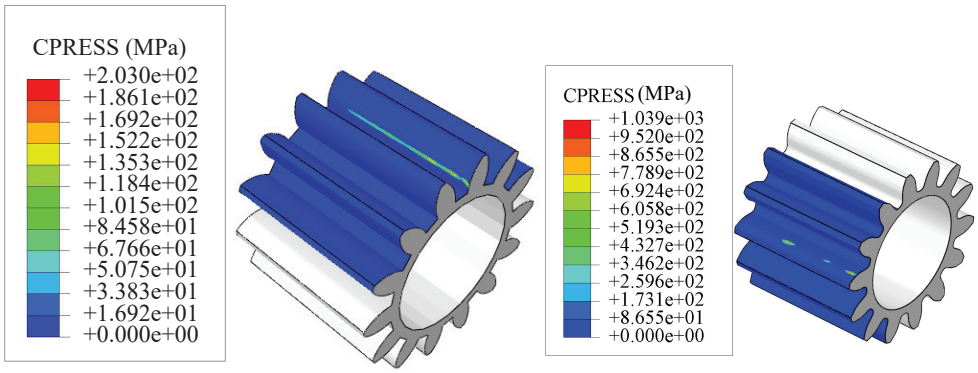
(**a**) (**b**)

Figure 15. NURBS interpolated 3D surfaces of gear and pinion (The colors only represent changes in height in the *z*-direction and have no other special meanings). (**a**) Gear. (**b**) Pinion.

4.2. Finite Element Analysis of Measured Gears

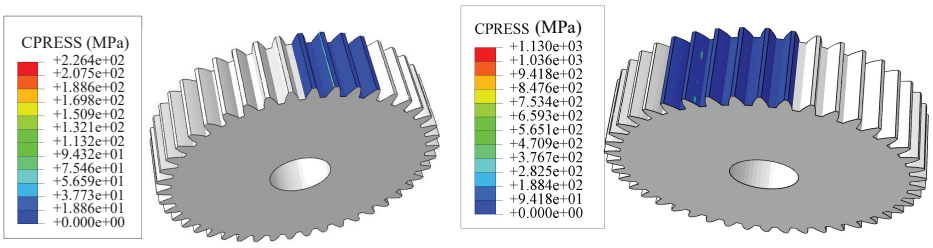
This section is to evaluate the contact stresses on the measured gear pairs. Although the measurement experiments were performed for only one gear pair, the finite element calculation was performed for the three-stage gear system. The applied torque load at the output end is 200 Nm, the friction coefficient is 0.2, and the rest of the finite element preprocessing method is similar to that of Section 3. For comparative analysis, Figures 16 and 17 report the maximum contact stress contours for the ideal and error gears. Because finite element software like ABAQUS has no unit information when inputting material parameters, load parameters, etc., the users only need to input a numerical value. However, the users need to ensure consistency in the dimensions of the input data for each physical quantity and know the units of the calculation results. To better understand Figures 16 and 17, the authors manually added the units MPa.

Attending to Figures 16 and 17, the contact stresses are uniform along the face width direction for the ideal pinion and gear, while for the error pinion and gear, the contact stresses are discontinuous. The results of the stress comparison between the two figures are presented in Table 10.



(**a**) (**b**)

Figure 16. Contact stress contours of pinion along face width direction. (**a**) Ideal pinion. (**b**) Error pinion.



(**a**) (**b**)

Figure 17. Contact stress contours of gears along face width direction. (**a**) Ideal gear. (**b**) Error gear.

Table 10. Comparisons of contact stresses between ideal gears and error gears.

Parameters	Ideal Pinion	Error Pinion	Multiple	Ideal Gear	Error Gear	Multiple
CPRESS/MPa	203	1039	5.12	226.4	1130	4.99

To further illustrate the relationship between tooth profile error and contact stress distribution, Figure 18 is introduced. It depicts the distribution of tooth profile error along the face width z direction for the gear's measurement data (one of the rows), where the red line indicates no error and the blue line refers to the tooth profile error. Combining Table 10 and the stress distribution state of the gears, it can be concluded that the distribution law of the contact stress is related to the distribution law of the tooth profile error. The maximum contact stress will appear where the tooth flanks are convex or concave, that is, where the tooth profile error is greatest. The existence of local maximum contact stress will increase the gear wear. Therefore, studying systematic and random errors can enable us to reduce these two types of errors at the machining stage by means of tooth profile modification and other methods.

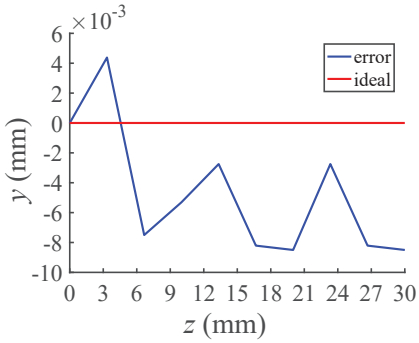


Figure 18. Distribution of tooth profile error along face width direction based on measurement data.

5. Discussion

The purpose of our study is to propose a modeling method for involute tooth profile error, which can simulate the actual tooth flanks formed by gear machining errors. The systematic errors formed by different gear machining processes are different, and the tooth profile form errors formed by the same machining method are also different due to different random errors. The actual involute tooth profile formed by the above reasons can only be determined through modeling within the tooth profile tolerance. In summary, when designing a gear transmission system, if the machining process of this gear and the variations in its base circle radius and rolling angle are known, the accurate tooth profile of the gear can be simulated using the modeling method proposed in this paper, and a three-dimensional solid error model of the gear can be established. Through methods such as finite element calculations, we can obtain more realistic transmission accuracy. Especially for fine-pitch precision gears, the impact of systematic and random errors during the machining process is more significant due to the smaller allowable range of tooth profile tolerance, tooth profile slope deviation, and tooth profile form error. At this point, if we need to predict the transmission performance of the fine-pitch gear systems at the design stage, the superiority of the method proposed in this paper can also be demonstrated.

On the other hand, tooth profile errors will aggravate tooth wear and affect the transient transmission error of gears. To minimize these effects, some measures should be taken. For mass-produced gears, it is impossible to measure each gear, but we can measure a few gears to find the systematic error that conforms to the machining law. Then, the tooth profile modification can be utilized to remove that systematic error. For precision gears processed in small quantities, due to the small quantity, we can measure each gear to find systematic and random errors. At this point, the systematic and random errors can be removed by profile modification. Therefore, the benefit of the involute profile error modeling proposed in this paper is that we must first understand the systematic and random errors formed during machining and then eliminate them as much as possible. Moreover, for precision complex transmission systems that involve a large number of gears, according to the meshing error calculation method proposed in this paper, the quantitative impact of each pair of gears on the transmission error of the whole transmission system can be determined, which is conducive to the optimization design of essential gears.

6. Conclusions

This paper investigates the effects of distributed tooth profile errors (including systematic and random errors) on the transmission accuracy and contact stress of a complex transmission system. The systematic error is mainly caused by the pressure angle deviation. The random error is primarily caused by the variation in base circle radius and the variation in rolling angle, and their mathematical models are established, respectively. Then, the finite element contact dynamic model is established. In view of the simulation results, the contact stresses of the fixed-axis gear train are compared with the calculated contact stresses to illustrate the impact of the distributed tooth profile errors on the contact stresses. Furthermore, based on the numerical simulation model, we propose a calculation method for the gear meshing error. According to the calculation results, we have found that non-uniform tooth profile errors will increase the variation in transient transmission errors, thereby affecting gear transmission errors.

The main conclusions of this study are summarized as follows.

(1) Since the pressure angle at each point on the involute is not equal, the positional error of the involute due to systematic errors in gear machining can be expressed as a function of the variation in the pressure angle. The change in the tooth profile form of the involute due to random errors in gear machining can be expressed as a function of the change in base circle radius and the change in roll angle. These are presented in the modeling of involute profile errors proposed in this paper.

(2) Compared with the calculated contact stresses obtained by the formulas, the contact stresses with distributed tooth profile error are relatively higher. Through experimental

verification, we have determined that the contact stresses are non-uniformly distributed along the face width direction and the maximum contact stresses appear in the convex and concave positions of the tooth surface. Moreover, the transmission error with distributed tooth profile error is larger than the transmission error without considering the tooth profile error previously studied by the authors. Furthermore, comparing the transmission errors under the influence of temperature with the transmission errors considering only tooth profile errors, it is found that temperature exacerbates the meshing error fluctuations.

(3) The gear meshing error extraction method proposed in this paper can further obtain the transmission error of the gear system, thereby determining the meshing gear pairs that have the most significant impact on the transmission accuracy of the system. For instance, according to the results of the analysis of transmission accuracy in this paper, the meshing error formed by gears 5 and 7 is the governing factor affecting the transmission error. This result is consistent with the sensitivity analysis in the authors' previous study.

Author Contributions: Conceptualization and methodology, M. Z., Z.Z. and J.X.; writing—original draft, M.Z.; writing—review and editing, M.Z. and J.X.; formal and resources, X.C.; software and validation, M.Z.; supervision, Z.Z. All authors have read and agreed to the published version of the manuscript.

Funding: This research was funded by the National Natural Science Foundation of China (grant numbers U22B2088, 52205512, and 52305530).

Data Availability Statement: Data are contained within the article.

Conflicts of Interest: The authors declare no conflicts of interest.

References

1. Wang, J.; Wang, S.; Ma, C.; Xia, C. Crucial errors identification of worm grinding process of face gears based on tooth flank posture error model and their influences on tooth flank errors. *Int. J. Adv. Manuf. Technol.* **2022**, *119*, 6177–6192. [CrossRef]
2. Karma, V.K.; Maheshwari, G. *Determination of Transmission Error and Mesh Stiffness in Spur Gear Pair Using CAD-FEM Integration Approach*; IOP Publishing Ltd.: Tamil Nadu, India, 2023. [CrossRef]
3. Pedrero, J.I.; Sánchez, M.B.; Pleguezuelos, M. Analytical model of meshing stiffness, load sharing, and transmission error for internal spur gears with profile modification. *Mech. Mach. Theory* **2024**, *197*, 105650. [CrossRef]
4. Velex, P.; Chapron, M.; Fakhfakh, H.; Bruyère, J.; Becquerelle, S. On transmission errors and profile modifications minimising dynamic tooth loads in multi-mesh gears. *J. Sound Vib.* **2016**, *379*, 28–52. [CrossRef]
5. Chen, H.; Zhu, Y.; Mao, J.; Wang, X. Influence of tooth profile modification on design transmission error of involute spur gear. *J. Huazhong Univ. Sci. Technol. (Natural Sci. Ed.)* **2018**, *46*, 91–97. [CrossRef]
6. Sanchez, M.B.; Pleguezuelos, M.; Pedrero, J.I. Influence of profile modification on the transmission error of spur gears under surface wear. *Mech. Mach. Theory* **2024**, *191*, 105473. [CrossRef]
7. Chen, Z.; Ji, P. Research on the variation of mesh stiffness and transmission error for spur gear with tooth profile modification and wear fault. *Eng. Fail. Anal.* **2020**, *122*, 105184. [CrossRef]
8. Zhou, D.; Guo, Y.; Yang, J.; Zhang, Y. Study on the Parameter Influences of Gear Tooth Profile Modification and Transmission Error Analysis. *Machines* **2024**, *12*, 316. [CrossRef]
9. Zhang, M.; Zhang, Z.; Shi, L. A new assembly error modeling and calculating method of complex multi-stage gear transmission system for a large space manipulator. *Mech. Mach. Theory* **2020**, *153*, 103982. [CrossRef]
10. Ottewill, J.R.; Neild, S.A.; Wilson, R.E. An investigation into the effect of tooth profile errors on gear rattle. *J. Sound Vib.* **2010**, *329*, 3495–3506. [CrossRef]
11. Tuplin, W.A. *Gear Design*, 1st ed.; Machinery Publishing Co. Ltd.: London, UK, 1962.
12. Xun, C.; Long, X.; Hua, H. Effects of random tooth profile errors on the dynamic behaviors of planetary gears. *J. Sound Vib.* **2018**, *415*, 91–110. [CrossRef]
13. Gregory, R.W.; Harris, S.L.; Munro, R.G. Dynamic Behaviour of Spur Gears. *Proc. Inst. Mech. Eng.* **1963**, *178*, 207–226. [CrossRef]
14. Theodossiades, S.; Natsiavas, S. Periodic and chaotic dynamics of motor-driven gear-pair systems with backlash. *Chaos Solitons Fractals* **2001**, *12*, 2427–2440. [CrossRef]
15. Özgüven, H.; Houser, D.R. Dynamic analysis of high speed gears by using loaded static transmission error. *J. Sound Vib.* **1988**, *125*, 71–83. [CrossRef]
16. Mark, W.D. Use of the generalized transmission error in the equations of motion of gear systems. *J. Mech. Des. Trans. ASME* **1987**, *109*, 283–291. [CrossRef]
17. Liu, C.; Qin, D.; Liao, Y. Dynamic model of variable speed process for herringbone gears including friction calculated by variable friction coefficient. *J. Mech. Des. Trans. ASME* **2014**, *136*, 041006. [CrossRef]

18. Yuan, B.; Chang, S.; Liu, G. Quasi-static analysis based on generalized loaded static transmission error and dynamic investigation of wide-faced cylindrical geared rotor systems. *Mech. Mach. Theory* **2019**, *134*, 74–94. [CrossRef]
19. Yuan, B.; Chang, L.; Liu, G. An efficient three-dimensional dynamic contact model for cylindrical gear pairs with distributed tooth flank errors. *Mech. Mach. Theory* **2020**, *152*, 103930. [CrossRef]
20. Bonori, G.; Pellicano, F. Non-smooth dynamics of spur gears with manufacturing errors. *J. Sound Vib.* **2007**, *306*, 271–283. [CrossRef]
21. Wang, Q.; Zhang, Y. A model for analyzing stiffness and stress in a helical gear pair with tooth profile errors. *J. Vib. Control.* **2016**, *23*, 272–289 . [CrossRef]
22. Wang, Q. An Investigation for Analyzing the Dynamic Characteristics and Fatigue Reliability of a Gear System. Ph.D. Thesis, Northeast University, Shengyang, Liaoning Province, China, 2015.
23. Chen, Z.; Zhou, Z.; Zhai, W. Improved analytical calculation model of spur gear mesh excitations with tooth profile deviations. *Mech. Mach. Theory* **2020**, *149*, 103838. [CrossRef]
24. Chen, Z.; Shao, Y. Mesh stiffness calculation of a spur gear pair with tooth profile modification and tooth root crack. *Mech. Mach. Theory* **2013**, *62*, 63–74. [CrossRef]
25. Kim, B.S.; Jeong, S.T.; Ahn, H.J. The Prediction of the angular transmission error of a harmonic drive by measuring noncontact tooth profile and considering three-dimensional tooth engagement. *Int. J. Precis. Eng. Manuf.* **2023**, *24*, 371–378. [CrossRef]
26. *GB/T 10095.1-2022*; Shi, Z.; Wang, Z.; Yu, B. Cylindrical gears-ISO System of Flank Tolerance Classification—Part 1: Definitions and Allowable Values of Deviations Relevant to Flanks of Gear Teeth. State Administration for Market Regulation and Standardization Administration of China, CNKI, Beijing, China, 2022.
27. Liu, X. (Ed.) *Involute Cylindrical Gear*; China Planning Press: Beijing, China, 2004.
28. Zhang, Z.; Zhang, Z.; Jin, X. A novel modelling method of geometric errors for precision assembly. *Int. J. Adv. Manuf. Technol.* **2017**, *94*, 1139–1160. [CrossRef]
29. *GB/T 3480-1997*; Calculation Methods of Load Capacity for Involute Cylindrical Gears. State Technology Supervision Administration, CNKI: Beijing, China, , 1997.
30. Hertz, H. Uber die beruhrung fester elastlseher korper. *Reine Angew. Math.* **1882**, *92*, 156–171. [CrossRef]
31. Zhang, Q.; Zhang, Z.; Jin, X.; Zeng, W. Entropy-based method for evaluating spatial distribution of form errors for precision assembly. *Precis. Eng.* **2019**, *60*, 374–382. [CrossRef]
32. Zhang, Q.; Xin, J.; Zhihua, L.; Zhang, Z. A new approach of surfaces registration considering form errors for precise assembly. *Assem. Autom.* **2020**, *40*, 789–800. [CrossRef]
33. Zhang, Q. Research on Assembly Accuracy Prediction for Precision Instruments. Ph.D. Thesis, School of Mechanical Engineering, Beijing Institute of Technology, Beijing, China, 2020.
34. Guo, H.; Zhang, Z.; Xiao, M.; Liu, H. Tolerance optimization method based on flatness error distribution. *Int. J. Adv. Manuf. Technol.* **2021**, *113*, 279–293. [CrossRef]
35. Ding, H.; Zhu, L.; Xiong, Z. Survey on coordinate measurement, geometric modeling and RP or NC generation from measured data points. *Chin. J. Mech. Eng.* **2003**, *39*, 10. [CrossRef]

Disclaimer/Publisher's Note: The statements, opinions and data contained in all publications are solely those of the individual author(s) and contributor(s) and not of MDPI and/or the editor(s). MDPI and/or the editor(s) disclaim responsibility for any injury to people or property resulting from any ideas, methods, instructions or products referred to in the content.